Re-measuring recrystallized grain sizes in quartz shearing experiments

Renée Heilbronner, Basel and Tromsø University (renee.heilbronner@unibas.ch)
Rüdiger Kilian, Basel University (ruediger.kilian@unibas.ch)
Jan Tullis, Brown University (jan_tullis@brown.edu)

1 - Experiments

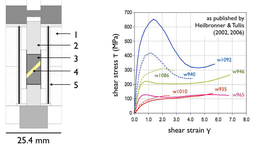

General shear experiments on Black Hills quartzite.
(a) Simplified drawing of sample assembly for general shear experiments: 1 = confining medium (NaCl), 2 = axial load/ σ1 piston (Al2O3), 3 = forcing block (Al2O3), 4 = quartzite sample at 45° with respect to σ1 piston, 5 = furnace (carbon, pyrophyllite)
(b) Shear stress (τ) versus apparent shear strain (γ): blue = regime 1, green = regime 2, red = regime 3, stippled line = relatively low finite strain, solid line = relatively high finite strain (compare Table 1).

2 - Previous results

Grain size of regime 1, 2, 3

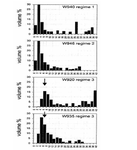

Sample # (regime)	Vol % recryst.	Vol % annealed	Modif. grain diameter (µm)
w871 (1)	50		5
w872 (2)	60		7
w858 (3)	85		20
w875 (1 anim.)		100	20
w873 (2 anim.)		100	30
w868 (3 anim.)		100	50
w940 (1)	50		7
w946 (2)	90		7
w929 (3)	100		14
w933 (3)	100		14

(Heilbronner & Tullis 2002)
Results of analyses

(Heilbronner & Tullis 2002)
Grain size distribution of samples deformed by shearing, plotted as volume % versus radius of volume equivalent sphere. 2D grain boundary maps were prepared form misorientation images (magnification 10x). Arrows indicate mode of recrystallized grain size.

Textures

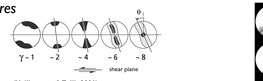

(Heilbronner & Tullis 2006)
Relation of c axis pole figure evolution to volume percent recrystallization. Schematic of c axis pole figure development. Bulk pole figures (of porphy- roclasts and recrystallized grains) as a function of increasing sinistral shear strain. Shear plane is horizontal and σ1 is oriented at 45°; the straight line is the fabric skeleton axis.

(Heilbronner & Tullis 2002)
Bulk c-axis pole figures of samples deformed by shearing. Measured area = 0.4 mm². Contours 0.5 times uniform.

Grain size of Y-domain

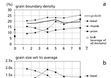

(Heilbronner & Tullis 2006)
Grain boundary density and relative grain size in different c axis domains as a function of strain. (a) Grain boundary density of different c axis orientation domains as a function of increasing shear strain and recrystallization.The data point at zero strain refers to the starting BHQ. The heavier line (=30° grids) represents the sum of all three orientation domains whose trends are shown separately. (b) Grain size (with respect to the average grain size) derived by inverting the grain boundary density. Rhomb and prism domains are fully recrystallized at γ = 1.5, whereas the basal domain is not fully recrystallized until γ ~ 5.

(Heilbronner & Tullis 2006)
Optical micrographs (using circular polarization) illustrating the difference in recrystallized grain size between the prism, the rhomb, and other domains. Details of samples with low and high volume percent recrystallization are shown. (a) W920 with γ ~ 1.5. (b) Prism domain of W935 with γ ~ 6. Grains of the prism domain appear black; grains of the rhomb domain are gray and grains of the basal domain light. Note larger size of prism grains (arrow in Figure 13a) compared to grains of other orientations.

3 - Orientation imaging

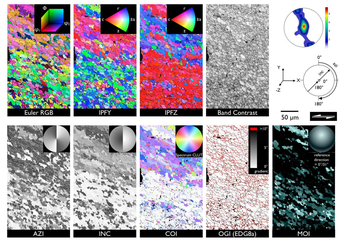

Orientation images.
(a) EBSD maps with color look-up tables (CLUT)
Euler RGB Euler coloring with Red = φ1, Green = Φ, Blue = φ2 (see CLUT).
IPFY, IPFZ Inverse pole figure coloring with respect to Y and Z (see CLUT).
(b) c-axis orientation images with look-up tables (LUT).
AZI, INC c-axis azimuth (0°-180°) and inclination (0°-180°) images calculated from Euler image, stereographic projection of LUT in upper right.
COI c-axis orientation image using Spectrum CLUT.
OGI c-axis orientation gradient image (EDGBs) showing average gradient with respect to 8 neighbours (see LUT).
MOI c-axis misorientation image: pixels with c-axis close to reference direction 0°/31° appear bright (see CLUT).
Upper right: c-axis pole figure, with (left-handed) XYZ sample coordinate system and coordinate system for c-axis orientation. Note that Z of this reference system is parallel to the structural Y direction. Scale bar and sinistral shear sense apply to all.
Detail of sample w965 is shown. For image processing, see text.

4 - EBSD and CIP

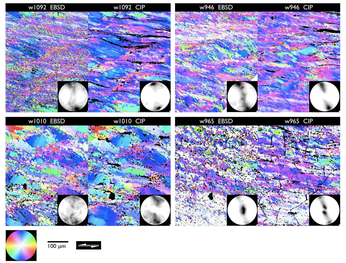

Comparison of c-axis orientation images calculated with CIP from optical or EBSD derived input.
EBSD c-axis orientation image from EBSD input (SEM),
CIP c-axis orientation image from CIP input (polarization microscopy).
Spectrum CLUT for c-axis color coding, scale and shear sense apply to all.
With exception of w946, the exact same sampling sites are shown for each pair.

5 - Grain size

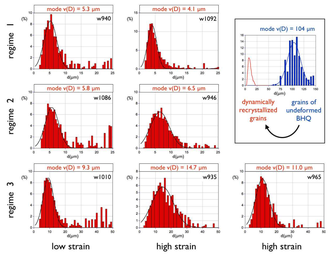

Recrystallized grain size for dislocation creep regimes 1, 2, and 3.
Volume weighted histograms v(D) are shown for 7 samples for relatively low (2.7 < γ < 4.3) and high shear strains (5.8 < γ < 7.1).
D = diameter of volume equivalent sphere. The mode of v(D) is obtained by a Gauss fit to the distribution.
Note histograms with different size ranges: (0 < D < 25 µm) for regime 1 and 2, (0 < D < 50 µm) for regime 3.
Inset shows the grain size distribution of undeformed Black Hills quartzite for comparison.
(Shear strain values as in original paper).

Map	Number of grains	Mode v(D)	Standard deviation	μ + σ	μ + 2σ	μ + 3σ	RMS(d)
undeformed Black Hills Quartzite							
BHQ undef. EBSD	216	104.1200	5.3856	109.51	114.89	120.28	77.214
BHQ undef. CIP	1146	103.9600	13.847	117.81	131.65	145.50	89.964
(c) all maps							
1a-w940	5914	5.2979	1.9958	7.2937	9.2895	11.29	4.1186
1b-w1092	34115	4.0942	0.4419	5.5361	6.9820	8.43	3.4035
1b-w1092-s30	9871	4.0790	1.4839	5.5629	7.0467	8.53	3.3308
2a-w1086	4377	5.7705	2.1522	7.9227	10.075	12.23	4.9579
2b-w946	19279	6.5384	2.9552	9.4936	12.439	15.39	4.5242
3a-w1010-s34	6441	9.0813	3.4139	12.495	15.909	19.32	7.9589
3a-w1010-s36	5793	9.2756	3.4170	12.693	16.110	19.53	8.3934
3b-w935	13554	14.5450	6.5298	21.073	27.603	34.13	9.3815
3b-w965-s40	10910	10.9640	4.3534	15.317	19.671	24.02	7.5841
3b-w965-s45	1860	10.0500	4.3044	14.354	18.659	22.96	6.6653
(b) dependence on grain kernel average misorientation (gKAM)							
1b-w1092-high gKAM	19391	3.9213	1.3561	5.2774	6.6335	7.99	3.2697
1b-w1092 low gKAM	14725	4.2960	1.5167	5.8127	7.3295	8.85	3.5699
2b-w946 high gKAM	13406	5.6628	2.4508	8.1136	10.564	13.02	4.0418
2b-w946 low gKAM	6396	7.7984	3.1009	10.899	14.000	17.10	5.4014
3b-w935 high gKAM	7898	13.0990	5.8398	18.939	24.779	30.62	8.6666
3b-w935 low gKAM	6220	16.2140	7.1071	23.321	30.428	37.54	10.267
(c) texture dependence							
1b-w1092 all (center strip)	25553	4.2660	1.4415	5.7075	7.1490	8.59	3.4041
1b-w1092 B-domain	11647	4.6881	1.8084	6.4965	8.3048	10.11	3.4741
1b-w1092 Y-domain	2289	4.1495	1.2075	5.3570	6.5646	7.77	3.2928
2b-w946 all	19280	6.5776	2.9357	9.5133	12.449	15.38	4.5241
2b-w946 B-domain	7425	7.2038	3.3556	10.559	13.915	17.27	4.7579
2b-w946 Y-domain	5634	6.5537	2.8060	9.3597	12.166	14.97	4.4397
3b-w965 all	10910	11.0140	4.3210	15.335	19.656	23.98	7.5828
3b-w965 B-domain	2203	11.5460	4.8128	16.359	21.172	25.98	7.8153
3b-w965 Y-domain	7385	11.0500	4.2983	15.348	19.647	23.94	7.6113
3b-w935 all	13559	14.6840	6.8181	21.502	28.320	35.14	9.3800
3b-w935 B-domain	2817	14.1530	6.8713	21.024	27.895	34.77	9.1574
3b-w935 Y-domain	7702	15.972	7.0684	22.413	29.482	36.55	9.5594

Table Grain size measurements.
1 Processed maps: prefix 1, 2, 3 indicates regime 1, 2, 3; a, b indicates low, high shear strain
2 Number of grains with >75% of pixels indexed
3 Mode of v(D) where v = volume weighted distribution and D = diameter of recalculated 3-D grains (volume equivalent spheres) = mean of Gaussian fit
4 Standard deviation of Gauss fit
5 Mean of Gaussian fit + 1 standard deviation = upper limit that includes 67% of population of 3-D grains
6 Upper limit including 84% of population of 3-D grains,
7 Upper limit including 99% of population of 3-D grains,
8 Root mean square of frequency distribution of diameter of 2-D sections h(d) where h = number density and d = diameter of 2D grains (area equivalent circles)

EBSD map obtained by electron back scatter diffraction
CIP map obtained by computer integrated polarization microscopy
B-domain pixels with c-axis maximum at periphery of pole figure
Y-domain pixels with c-axis maximum in center of pole figure

6 - Texture dependent grain size

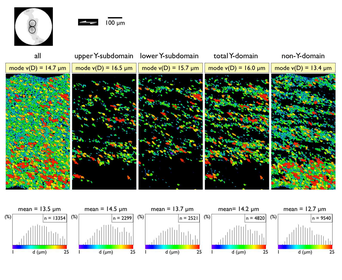

Mapping grain size in texture domain.
Grain size maps of detail of sample w935 (regime 3) are shown. From left to right: showing all grains, grains in the upper and lower Y-subdomains, in the whole Y-domain and for c-axis orientations outside the Y-domain (see c-axis pole figure), same subdomains as in Figure 7. Domain maps are derived for c-axes orientations within a 30° cone (15° opening angle) with respect to the central orientation. Scale bar and shear sense apply to all.
Above maps:
Modes of v(D) are indicated above maps, where v = volume density distribution, D = diameter of volume equivalent sphere.
Below maps:
Histograms showing area weighted distributions of grain size (= grey value histogram of gain size map, see Heilbronner & Barrett, 2014 chap. 12), n = number of grains, mean = arithmetic mean of histogram. Note that the grain size in the Y-domains is larger than in the non-Y-domain, but the difference between upper and lower Y-subdomain is not considered significant.

7 - Grain KAM dependent grain size

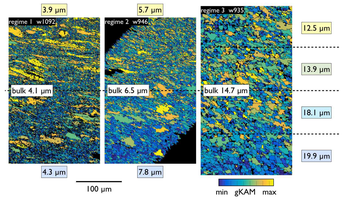

Recrystallized grain size as function misorientation density.
Maps of grain kernel average misorientation (gKAM) are shown for 3 dislocation creep regimes. Maps cover nearly the full width of the shear zone. Gradients of gKAM are clearly visible. Modes of v(D) (size distribution of 3D grains) are calculated for high and low gKAM sites in samples w1092 and w946, and for 4 different sites of sample w935.
Scale bar and color coding of gKAM apply to all.

8 - Double c-axis maxima

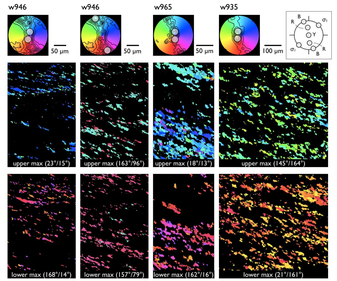

Details of c-axis texture.
Color coded orientation images highlighting 'double maxima' c-axis orientations.
(a) Contoured polefigures superposed on the AZI color look-up-table (CLUT) used to highlight the azimuth of the c-axis orientation.
Inset: Location of preferred orientations on the c-axis pole figure, proposed by Heilbronner & Tullis (2006): B ('basal'), R ('rhomb'), Y ('prism') and the direction of the axial load (at 45° with respect to the shear zone, usually inferred to be the direction of σ1).
(b) Masked c-axis orientation images. Mask blocks all pixels with c-axis orientations outside a 30° cone (15° opening angle) about the reference direction. The reference direction is indicated below the image and corresponds to the upper maximum on the pole figure shown in (a).
(c) Same as (b) with the reference direction indicated below the image corresponding to the lower maximum on the pole figure shown in (a).

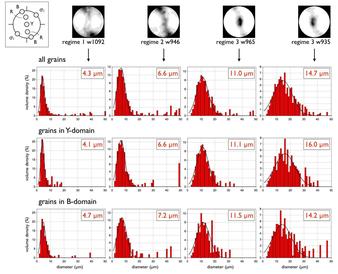

Recrystallized grain size as function of texture.
Grain size distributions of recrystallized grains for four samples of regime 1, 2, and 3 of dislocation creep, arranged in 4 columns with c-axis pole figure above.
(a) Grain size distributions of all recrystallized grains.
(b) Grain size distributions of recrystallized grains with c-axis orientations within 30° cone (15° opening angle) about Y direction.
(c) Same as (b) for B direction.
Inset (upper left) shows location of c-axis orientations of B- and Y-domain on the pole figure.

Literature
Heilbronner, R. and Kilian, R. (subm). EGU Solid Earth (in discussion)
Heilbronner, R., and J. Tullis (2006), J. Geophys. Res., 111, B10202, doi:10.1029/ 2005JB004194.
Heilbronner, R. and Tullis, J. (2002). In: S. de Meer, et al. (Editors). Geol. Soc., Lond., Spec. Pub., pp. 191-218.
Kilian, R. and Heilbronner, R. (subm). EGU Solid Earth (in discussion)
Richter, B., Stünitz H. and Heilbronner R. (2016), J. Geophys. Res. Solid Earth, doi: 10.1002/2016JB013084.
Stipp, M., and J. Tullis (2003), Geophys. Res. Lett., 30(21), 2088, doi:10.1029/2003GL018444.

9 - Piezometer relationships

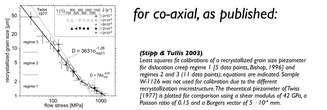

for co-axial, as published:

(Stipp & Tullis 2003).
Least squares fit calibrations of a recrystallized grain size piezometer for dislocation creep regime 1 (5 data points, Bishop, 1996) and regimes 2 and 3 (11 data points); equations are indicated. Sample WI-1126 was not used for calibration due to the different recrystallization microstructure. The theoretical piezometer of Twiss [1977] is plotted for comparison using a shear modulus of 42 GPa, a Poisson ratio of 0.15 and a Burgers vector of 5 · 10⁻¹⁰ mm.

for shearing experiments of Black Hills quartzite

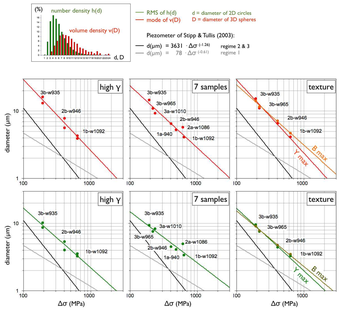

Recrystallized grain size as function of flow stress.
Two measures of average grain size are plotted against differential stress, Δσ (with Δσ = 2 · τ, see Table 1).
Top row: Mode of v(D), where D = diameter of volume equivalent sphere, and v = volume weighted frequency distribution (=3-D mode).
Bottom row: Root-mean-square of h(d), where d = diameter of area equivalent circle, and h = frequency distribution, as used for the piezometer relation by Stipp & Tullis (2003) (= 2-D RMS).
(a) High strain experiments (5.8 < γ < 7.1): in each case, higher value from low gKAM region, lower value for high gKAM region (see Figure 6).
(b) One measurement for each experiment (see Figure 1, Table 1).
(c) Grain sizes of Y- and B-domains (see Figure 7, 8)

for shearing experiments of quartz gouge

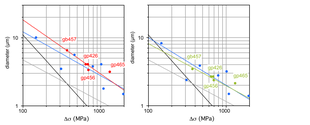

Preliminary / unpublished data on quartz gouge on:
Recrystallized grain size of quartz gouge deformed under general shearing conditions.
Left: Mode of v(D)
Right: Root-mean-square of h(d), both as above.
Red and green = data by **Giulia Pallazzin** (see EGU2017-4953 abstract, 2017)
Blue = data by **Bettina Richter** (see Richter et al, this conference)

Acknowledgements
Bettina Richter, Giulia Pallazzin, Hugues Raimbaud and Holger Stünitz for contributing grain size data of experimentally sheared quartz gouge.
Dave Prior and Michael Stipp for discussions.

Samples and Methods

1 For a series of shearing experiments on Black Hills quartzite, the recrystallized grain size was re-measured using EBSD maps obtained with the ZEISS Merlin SEM and AZtec acquisition software recently installed at Tromsø University.

2 The original experiments were carried out at Brown University at temperatures from 850° to 915°, confining pressures of 1.5 to 1.58 GPa, a shear strain rate of 10^{-5} s^{-1}, and with and without 0.2 wt% water added. Deformation was in the dislocation creep regime, and the resulting shear stresses τ were between 100 and 320 MPa. In the original papers (Heilbronner & Tullis, 2002, 2006), grain size determinations were made using c-axis orientation images (CIP method).

3 When re-examining the three dislocation creep regimes, two or three samples with bulk shear strains of γ = 2 - 7 were analyzed for each regime.

Results

4 When visualized as c-axis orientation images, the EBSD maps and the CIP maps are basically the same, with the exception of the spatial resolution.

5 The determination of the recrystallized grain sizes confirms the approximate measurements made using CIP for regime 3.

6 The texture dependence of the recrystallized grain size in the one case investigated in 2006. Grain size of the Y-domain is larger than then the rest.

7 For a second sample deformed under almost identical conditions, but to higher strain, such a texture dependence cannot be observed. However, in both samples, small recrystallized grain sizes correlate with high grain kernel average misorientation (gKAM). Many samples show gradients of gKAM and corresponding gradients of grain size. Within zones of constant gKAM, the texture dependence of grain size varies according to the active deformation mechanisms, evolving with strain before a stable grain size is developed.

8 Closer inspection of the c-axis pole figures reveals double maxima with distinct recrystallized grain sizes.

9 In order to compare the results to the quartz piezometer of Stipp & Tullis (2003), the RMS of the 2-D equivalent diameter of the recrystallized grains was plotted against the differential stress, Δσ (= 2 · τ). Overall, a clear dependence of grain size on flow stress was found, independent of the amount of finite shear strain the sample had incurred.

However, the resulting piezometer relationship shows that under shearing conditions the flow stresses are higher (or the grain sizes larger) than would be predicted by the Stipp &Tullis piezometer. Whether the discrepancy is due to the different kinematic frame work (coaxial versus non-coaxial), the difference in finite strain, i.e., total amount of recrystallization, or due to different experimental conditions that may have led to the activation of different deformation mechanisms or different combinations of mechanisms, is still under investigation.